Biosynthesis of 2-Phenylethanol in Rose Petals Is Linked to the Expression of One Allele of *RhPAAS*[1]

Aymeric Roccia,[a,b,2] Laurence Hibrand-Saint Oyant,[c,2] Emilie Cavel,[a] Jean-Claude Caissard,[a] Jana Machenaud,[a] Tatiana Thouroude,[c] Julien Jeauffre,[c] Aurélie Bony,[a] Annick Dubois,[b] Philippe Vergne,[b] Judit Szécsi,[b] Fabrice Foucher,[c] Mohammed Bendahmane,[b] and Sylvie Baudino[a,3,4]

[a]Université Lyon, Université Saint-Etienne, Centre National de la Recherche Scientifique, Laboratoire de Biotechnologies Végétales appliquées aux Plantes Aromatiques et Médicinales, FRE 3727, F-42023 Saint-Etienne, France

[b]Laboratoire Reproduction et Développement des Plantes, Université Lyon, Ecole Normale Supérieure de Lyon, Université Claude Bernard Lyon 1, Centre National de la Recherche Scientifique, Institut National de la Recherche Agronomique, F-69342 Lyon, France

[c]Institut de Recherche en Horticulture et Semences, Agrocampus-Ouest, Institut National de la Recherche Agronomique, Université d'Angers, Structure Fédérative de Recherche 4207 Qualité et Santé du végétal, 49071 Beaucouzé, France

ORCID IDs: 0000-0002-4451-8798 (L.H.O.); 0000-0003-3498-5090 (J.M.); 0000-0002-8539-3709 (P.V.); 0000-0002-1630-803X (J.S.); 0000-0002-3693-7183 (F.F.); 0000-0003-1661-1060 (M.B.); 0000-0002-3367-172X (S.B.).

Floral scent is one of the most important characters in horticultural plants. Roses (*Rosa* spp.) have been cultivated for their scent since antiquity. However, probably by selecting for cultivars with long vase life, breeders have lost the fragrant character in many modern roses, especially the ones bred for the cut flower market. The genetic inheritance of scent characters has remained elusive so far. In-depth knowledge of this quantitative trait is thus very much needed to breed more fragrant commercial cultivars. Furthermore, rose hybrids harbor a composite genomic structure, which complexifies quantitative trait studies. To understand rose scent inheritance, we characterized a segregating population from two diploid cultivars, *Rosa* × *hybrida* cv H190 and *Rosa wichurana*, which have contrasting scent profiles. Several quantitative trait loci for the major volatile compounds in this progeny were identified. One among these loci contributing to the production of 2-phenylethanol, responsible for the characteristic odor of rose, was found to be colocalized with a candidate gene belonging to the 2-phenylethanol biosynthesis pathway: the *PHENYLACETALDEHYDE SYNTHASE* gene *RhPAAS*. An in-depth allele-specific expression analysis in the progeny demonstrated that only one allele was highly expressed and was responsible for the production of 2-phenylethanol. Unexpectedly, its expression was found to start early during flower development, before the production of the volatile 2-phenylethanol, leading to the accumulation of glycosylated compounds in petals.

Roses (*Rosa* spp.) are among the most important ornamental plants and have been used since antiquity for their beauty and scent. Hundreds of volatile molecules, belonging to different biosynthetic pathways, have been isolated from rose petals. The combination of these molecules makes up the characteristic rose scent bouquet. Monoterpene alcohols such as geraniol and phenylpropanoid-related compounds such as 2-phenylethanol (2PE) have been shown to contribute greatly to the typical rose scent. Many studies have been performed to investigate the various ways in which these major compounds are produced in petals. The biosynthetic pathway leading to 2PE production has been previously studied in detail (Fig. 1), and the key enzymes of the pathway have been identified: PHENYLACETALDEHYDE SYNTHASE (RhPAAS; Kaminaga et al., 2006; Sakai et al., 2007; Farhi et al., 2010) and PHENYLACETALDEHYDE REDUCTASE (PAR; Chen et al., 2011). Recently, an alternative pathway, which is seasonally induced in summer, has been identified in roses for the production of 2PE. This pathway uses AROMATIC AMINO ACID AMINOTRANSFERASE (Hirata et al., 2012) and PHENYLPYRUVATE DECARBOXYLASE (Hirata et al., 2016) to produce 2-phenylacetaldehyde (Fig. 1, dashed arrows). Monoterpene biosynthesis in rose has recently been

[1]This work was supported by funding from the Région Rhône-Alpes, Centre National de la Recherche Scientifique, and INRA, France. Additional support was provided by CNRS GDR MediatEC (3658) and ANR Rosascent.

[2]These authors contributed equally to the article.

[3]Author for contact: sylvie.baudino@univ-st-etienne.fr.

[4]Senior author.

The author responsible for distribution of materials integral to the findings presented in this article in accordance with the policy described in the Instructions for Authors (www.plantphysiol.org): Sylvie Baudino (sylvie.baudino@univ-st-etienne.fr).

S.B. conceived the original screening and research plans; S.B., J.-C.C., F.F., and M.B. supervised the experiments; A.R., L.H.-S.O., J.M., E.C., J.-C.C., and S.B. performed most of the experiments; T.T., J.J., J.S., P.V., A.B., and A.D. performed transformation and gene expression analyses and provided conceptual and/or technical assistance to A.R., E.C., and J.M.; S.B., M.B. and L.H.-S.O. designed the experiments; S.B. and L.H.-S.O. analyzed the data; S.B. conceived the project and wrote the article with contributions from all the authors.

www.plantphysiol.org/cgi/doi/10.1104/pp.18.01468

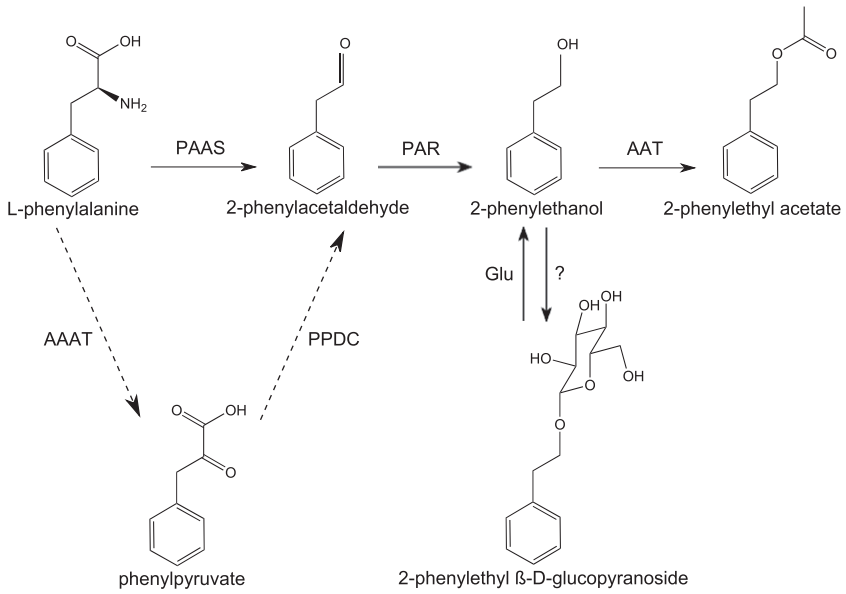

Figure 1. The 2PE biosynthetic pathway in roses. AAAT, AROMATIC AMINO ACID AMINOTRANSFERASE (*R. hybrida* cv Yves Piaget, *RyAAAT3* gene; Hirata et al., 2012); AAT, ACETYL-COENZYME A: GERANIOL/CITRONELLOL ACETYL TRANSFERASE (*R. hybrida* cv Fragrant Cloud, *RhAAT1* gene; Shalit et al., 2003); Glu, β-GLUCOSIDASE (*R. hybrida* cv Hoh-Jun, β-glucosidase enzyme; Sakai et al., 2008); PAAS, PHENYLACETALDEHYDE SYNTHASE (*R. hybrida* cv Fragrant Cloud, *RhPAAS* gene; Kaminaga et al., 2006; *R. hybrida* cv Hoh-Jun, *AADC* gene; Sakai et al., 2007); PAR, PHENYLACETALDEHYDE REDUCTASE (*R.* x *hybrida* cv Hoh-Jun, PAR enzyme; Sakai et al., 2007; *R. damascena*, *PAR* gene; Chen et al., 2011); PPDC, PHENYLPYRUVATE DECARBOXYLASE (*R.* x *hybrida* cv Yves Piaget, *RyPPDC* gene; Hirata et al., 2016); ?, putative glycosyltransferase, not yet characterized. Dashed arrows indicate an alternative pathway (Hirata et al., 2012).

deciphered. Roses, unlike other plants, use a nudix hydrolase to synthetize geraniol (Magnard et al., 2015). The biosynthetic pathway of 3,5-dimethoxytoluene (DMT) production, which is responsible for the tea scent of some cultivars, involves *O*-methyltransferases (Scalliet et al., 2006, 2008). These studies have generally shown that the genes are specifically expressed in petals when the scent is emitted and that the amount of volatile compounds is linked to the transcriptional level of the genes involved in the pathway (Farhi et al., 2010).

Despite these efforts, knowledge of rose fragrance biosynthesis is still incomplete and cannot yet be used to assist breeders in selecting scented roses. One of the reasons is that scent inheritance during crossings has seldom been evaluated in rose. Indeed, most studies have characterized the heritability of a wide range of other floral characteristics, such as resistance to pathogens, vigor, recurrence in flowering, inflorescence architecture, number of petals, and flower color (Linde et al., 2006; Yan et al., 2007; Kawamura et al., 2011; Henz et al., 2015; Roman et al., 2015; Gitonga et al., 2016; Bourke et al., 2018; François et al., 2018). Although genetic dissection of fruit aroma and flower scent in plants is difficult due to the nature and the number of compounds involved, such genetic studies, including quantitative trait locus (QTL) and genome-wide association studies, have been performed in some crop plants such as tomato (*Solanum lycopersicum*), for which powerful genetic resources exist (Rambla et al., 2017; Tieman et al., 2017). QTL approaches have also been applied to petunia (*Petunia* spp.) to study the evolution of floral scent in relationship to pollination syndrome (Klahre et al., 2011; Amrad et al., 2016). In Rosaceae, research efforts have been focused on the improvement of fruit flavor characters. Several studies have addressed the identification of QTLs for volatile compounds in apple (*Malus domestica*; Zini et al., 2005; Dunemann et al., 2012; Costa et al., 2013; Vogt et al., 2013; Souleyre et al., 2014; Yauk et al., 2015, 2017), raspberry (*Rubus* spp.; Paterson et al., 2013), and strawberry (*Fragaria* spp.; Zorrilla-Fontanesi et al., 2012). In strawberry and raspberry, the authors observed some genetic regions (clusters of QTLs) controlling several volatile compounds, suggesting either tightly linked multiple loci or single loci with pleiotropic effects, which could be coding for master regulators such as transcription factors or microRNAs. Genes likely responsible for some of the identified QTLs were sometimes assigned. In strawberry, the *O*-methyltransferase gene *FaOMT* was identified as the locus controlling natural variation in mesifurane content (Zorrilla-Fontanesi et al., 2012). In apple, candidate genes (coding for *O*-methyltransferases and alcohol acyltransferases), involved in the production of the phenylpropene estragole, were characterized (Yauk et al., 2017). In rose, the first published analysis of scent in a segregating population was performed on a crossing between tetraploid roses (Cherri-Martin et al., 2007). This analysis showed that a large proportion of descendants lacked volatile compounds of good fragrance value, so that this positive feature may have been lost in such a crossing. Another study of genetic determinism of rose compounds was conducted on diploid roses with a *Rosa multiflora* genetic background (Spiller et al., 2010). These authors resolved the patterns of inheritance for several important volatile compounds and were able to map six QTLs influencing volatile content. For example, they found two loci influencing the amount of 2PE. However, no functional relationships to known candidate genes in the 2PE pathway were found in that study.

The aim of this study was to identify genomic regions controlling scent compound production in rose petals. We addressed the genetic determinism of volatile compound production over 3 years in a diploid F1 progeny. We focused on the identification of the candidate gene responsible for the segregation of 2PE content in the population. Analyses of the alleles associated with the

production of 2PE and their expression during flower development were conducted.

RESULTS

Identification of Major Scent Loci

To study the inheritance of the production of scent in rose flowers, we performed gas chromatography (GC)-flame ionization detection and GC-mass spectrometry (MS) to analyze the volatile compounds in 79 individuals of the HW F1 progeny (named HW progeny; Crespel et al., 2002; Hibrand-Saint Oyant et al., 2008) during 3 successive years. To facilitate compound collection, we used a solvent solid/liquid extraction of petals in full-bloom flowers, which allowed us to analyze the free internal pool of petal volatile compounds. Thirty-nine compounds were recovered, including some nonvolatile long-chain hydrocarbons (Supplemental List). For further studies, the 16 most abundant volatile compounds were chosen. Compound measurements were made each year in the progeny and in the parents (Table 1). Striking differences in scent characteristics between the two parents were observed. The female parent, an *R.* x *hybrida* dihaploid cv H190 (H190), predominantly produced DMT and *E*-2-hexenal, while the male parent, an *R.* x *wichurana* hybrid (Rw), produced 2PE and *E*,*E*-farnesol at high concentrations. These results were consistent over all 3 years. On average, Rw produced 57.8 times more 2PE than H190. Extracts of both parents contained minor (i.e. less than 0.5 $\mu g\ g^{-1}$ fresh weight) compounds: 2-phenylacetaldehyde, 2-phenylethyl acetate, *E*-β-farnesene, farnesal, germacrene D, geraniol, geranyl acetate, and benzyl alcohol (Table 1). Some compounds were only detected in one parent, such as DMT and 2-phenylacetaldehyde in H190 and *Z*-3-hexenol, 2-phenylethyl acetate, farnesyl acetate, and geranyl acetate in Rw.

Correlations between the different scent compounds could indicate a common biosynthetic pathway. Therefore, we analyzed such correlations for each year and for the 3 years together (denoted by Y1, Y2, and Y3). The pairwise correlation for each volatile was analyzed against every other volatile, and the Spearman correlation coefficients were calculated. Some correlations were observed in more than 1 year (Supplemental Fig. S1). Volatile phenylpropanoid-related compounds and benzenoid compounds (2PE, 2-phenylacetaldehyde, 2-phenylethyl acetate, and benzyl alcohol) were positively correlated. The two apocarotenoid compounds dihydro-β-ionone and dihydro-β-ionol were also coregulated. The amounts of *E*-2-hexenal and *Z*-3-hexenol were negatively correlated. Other more unexpected pairwise positive correlations, such as the one implicating geraniol and *E*,*E*-farnesol, were also found in Y1 and Y2.

For most of the compounds, we observed a significant variance between genotypes and between years (Supplemental Table S1). Furthermore, as all the variances between technical replicates were weak or nonsignificant (except for farnesal) compared with the variances between genotypes and between years, we decided to average technical replicates and performed analyses on the means of these technical replicates. The heritability ranged from 28.4% to 96.12% (Supplemental Table S1). The highest heritability estimates were obtained for geranyl acetate (96.12%) and dihydro-β-ionol (87.92%). The smallest values of heritability were observed for benzyl alcohol, farnesal, and *E*-β-farnesene, 28.4%, 41.12%, and 45.13%, respectively.

Data obtained from each experiment (three experiments corresponding to 3 different years) were first used to perform a comprehensive QTL analysis for each parental map. For this analysis, we used the male and female genetic maps previously developed (Hibrand-Saint Oyant et al., 2008; Remay et al., 2009). Due to nonnormality distribution for most of the metabolites, the raw data were analyzed first by the nonparametric Kruskal-Wallis rank-sum test (KW). Interval mapping analysis (IM) was then performed with a step size of 1 centimorgan (cM) to find regions with potential QTL effects (i.e. where the logarithm of odds [LOD] score was greater than the threshold). The percentage explained by the QTL (r^2) was also presented. With KW, a total of 112 significant associations were detected for the 3 years (Supplemental Table S2). We assumed that associations detected in the same chromosomal region for the same volatile compound in different years were identical, and 77 QTLs were finally considered. Among them, 24 (31.2%) were stable over 2 or 3 years. Using IM, a total of 34 significant associations were obtained, resulting in 24 QTLs (Fig. 2; Table 2). Among them, eight (33.3%) were stable over 2 or 3 years. Moreover, some clusters of QTLs were detected in the same chromosomal regions (Fig. 2). All 24 QTLs detected with IM were also detected with KW (Supplemental Table S2). Data from the 3 years were then analyzed together by KW (Supplemental Table S3). Most of the 24 common QTLs detected in a single year by KW and IM were also detected when the data were averaged. Some QTLs were only detected when the data were averaged. Only the 24 QTLs detected by KW and IM are described below.

QTLs for fatty acid derivatives (*E*-2-hexenal Y1-Y2-Y3 and *Z*-3-hexenol Y2-Y3) were identified in the same region of the female map on Linkage Group (LG) 4, with a LOD score up to 6.1 for *E*-2-hexenal in Y2. These QTLs explained a large part of the variability observed for these compounds, between 25.1% and 41% (Table 2). A QTL for *E*-2-hexenal was also located on LG5 (B5) in Y1. It is noteworthy that these two compounds were negatively correlated (Supplemental Fig. S1).

On LG6 (B6), QTLs for phenylpropanoid-related compounds (2PE, 2-phenylacetaldehyde, and 2-phenylethyl acetate) were detected in the same region. Some LOD scores were up to 16.8 (e.g. 2PE in Y1). The detected QTL for 2PE explained more than 60% of the phenotypic variance, indicating a strong effect of this locus in the control of the variation of the trait. On the same locus, a QTL for benzyl alcohol was also detected in Y2

Table 1. *Mean and median values and range of volatile compounds (μg g^{-1} fresh weight, means of two to four replicates) analyzed by GC-flame ionization detection and GC-MS during three successive years (Y1, Y2, and Y3) in petals of Rw and H190 parental lines and in HW progeny*

Volatile Compound	Y1					Y2					Y3				
	HW Range	HW Mean ± SD	HW Median	H190	Rw	HW Range	HW Mean ± SD	HW Median	H190	Rw	HW Range	HW Mean ± SD	HW Median	H190	Rw
E-2-Hexenal	0.3–32.9	5.3 ± 0.7	3.7	8.3	0.4	0.7–37.0	8.1 ± 1.2	5.0	5.7	1.7	0.4–31.1	5.8 ± 0.8	4.0	14.9	0.8
Z-3-Hexenol	0.0–0.9	0.0 ± 0.0	0.0	0.0	1.4	0.0–14.8	2.1 ± 0.5	0.0	0.0	3.3	0.0–17.8	1.3 ± 0.4	0.0	0.0	1.9
2PE	0.0–350.5	65.5 ± 10.5	1.4	2.1	97.1	0.0–716.9	105.2 ± 23.8	0.9	1.2	183.9	0.0–487.9	73.1 ± 13.2	1.9	3.2	94.5
2-Phenylacetaldehyde	0–7.3	0.7 ± 0.2	0.0	0.2	0.0	0.0–14.4	1.2 ± 0.5	0.0	0.0	0.0	0.0–21.6	1.4 ± 0.5	0.0	0.0	0.0
2-Phenylethyl acetate	0.0–40.9	0.9 ± 0.5	0.0	0.0	0.5	0.0–2.5	0.2 ± 0.1	0.0	0.0	0.4	0.0–1.5	0.2 ± 0.0	0.0	0.0	0.2
3,5-Dimethoxytoluene	0.0–14.0	4.2 ± 0.4	3.5	25.9	0.0	0.2–33.0	6.3 ± 0.8	4.9	6.6	0.0	0.0–45.4	10.8 ± 1.2	8.2	14.9	0.0
Benzyl alcohol	0.0–1.1	0.3 ± 0.0	0.2	0.2	0.3	0.0–1.6	0.2 ± 0.1	0.0	0.0	0.4	0.0–0.8	0.1 ± 0.0	0.0	0.0	0.2
Geraniol	0.0–6.9	0.9 ± 0.2	0.4	0.1	0.2	0.0–2.8	0.3 ± 0.1	0.0	0.0	0.1	0.0–3.4	0.2 ± 0.1	0.0	0.0	0.0
Geranyl acetate	0.0–6.4	0.2 ± 0.1	0.0	0.0	0.3	0.0–1.9	0.1 ± 0.0	0.0	0.0	0.0	0.0–3.3	0.1 ± 0.1	0.0	0.0	0.0
Germacrene D	0.0–6.7	0.5 ± 0.1	0.1	0.0	0.2	0.0–1.0	0.1 ± 0.0	0.0	0.0	0.0	0.0–8.6	0.2 ± 0.1	0.0	0.0	0.0
E-β-Farnesene	0.0–4.2	0.7 ± 0.1	0.3	0.0	0.2	0.0–0.6	0.0 ± 0.0	0.0	0.0	0.0	0.0–1.9	0.1 ± 0.0	0.0	0.0	0.0
E,E-Farnesol	0.0–42.5	8.7 ± 1.3	1.8	1.1	19.0	0.0–25.0	6.1 ± 0.7	5.6	0.6	14.6	1.1–20.3	5.9 ± 0.5	5.3	2.4	12.6
Farnesal	0.0–1.2	0.2 ± 0.0	0.0	0.1	0.4	0.0–0.6	0.0 ± 0.0	0.0	0.0	0.0	0.0–1.3	0.3 ± 0.0	0.3	0.0	0.2
Farnesyl acetate	0.0–38.1	1.5 ± 0.6	0.4	0.0	4.9	0.0–1.7	0.0 ± 0.0	0.0	0.0	0.2	0.0–4.5	0.1 ± 0.1	0.0	0.0	0.9
Dihydro-β-ionone	0.0–3.2	0.5 ± 0.1	0.2	1.2	0.3	0.0–4.5	0.6 ± 0.2	0.0	1.9	0.0	0.0–4.6	0.7 ± 0.1	0.3	4.8	0.0
Dihydro-β-ionol	0.0–3.0	0.5 ± 0.1	0.4	0.7	0.6	0.0–6.4	1.0 ± 0.2	0.0	1.3	0.5	0.0–9.6	1.1 ± 0.2	0.4	2.1	0.7

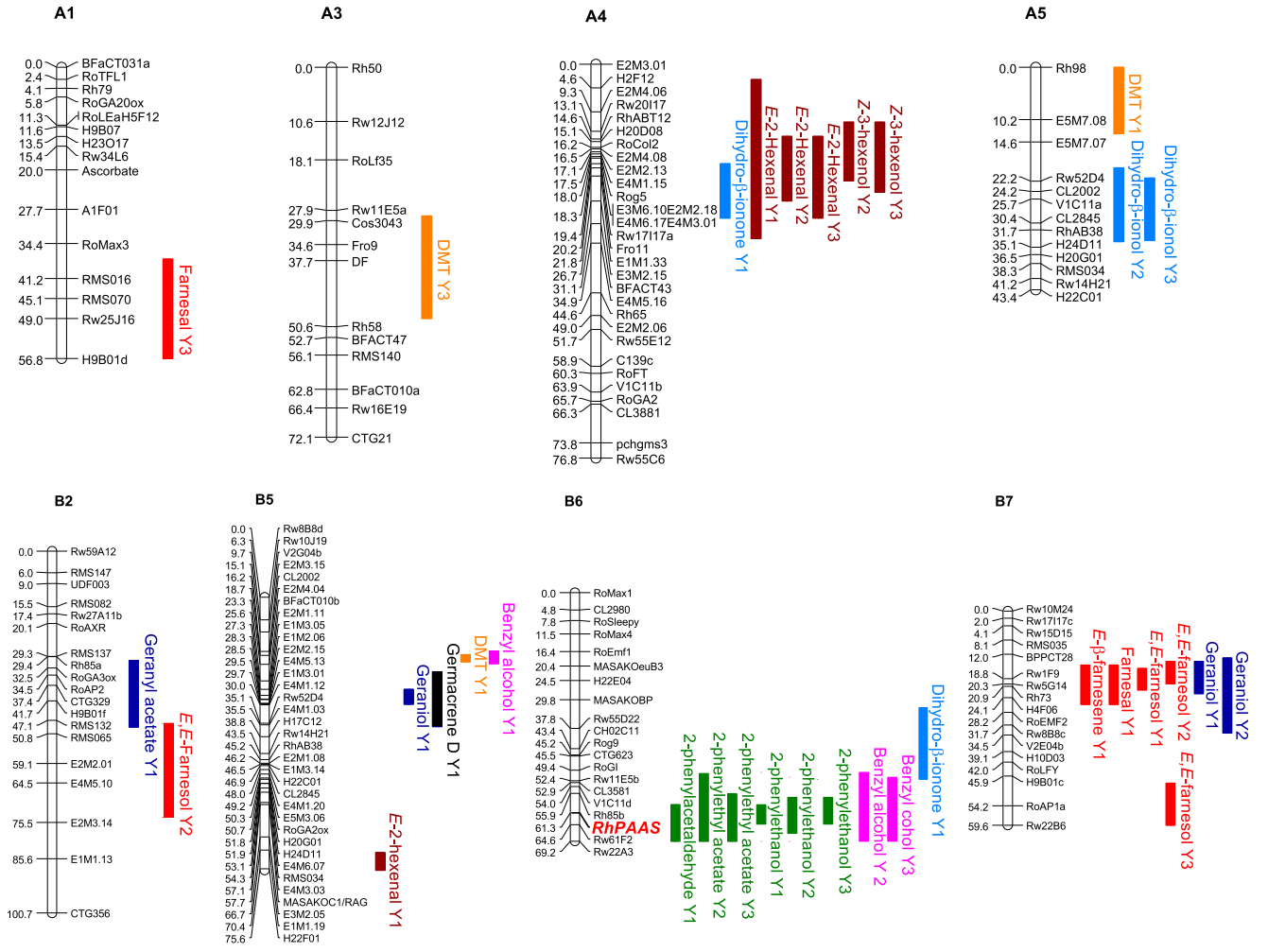

Figure 2. Locations of QTLs associated with scent compounds as determined by IM, and the major gene controlling 2PE production, *RhPAAS*, as candidate gene. The genetic linkage maps were constructed for both parents (female parent *R.* x *hybrida* cv H190, A1–A7, and male parent *R. wichurana*, B1–B7). QTLs associated with compounds are located to the right of the chromosomes, with color bars showing one-LOD confidence intervals.

and Y3. These four compounds showed a strong positive correlation (Supplemental Fig. S1). For benzyl alcohol, a QTL was also detected on LG5 (B5) in Y1.

On LG5 (A5 and B5), one QTL for DMT was detected in Y1 that explains 17.9% and 23.4% of variability, respectively. Another QTL for this compound was located in Y3 on LG3 (A3).

A cluster of QTLs was detected on the male LG7 (B7): one QTL for geraniol (Y1 and Y2), one QTL explaining up to 49.2% of the *E*,*E*-farnesol content in Y1 and Y2 (K value < 0.0001), and two QTLs for two other related compounds (*E*-*β*-farnesene in Y1 and farnesal in Y1). Another QTL for *E*,*E*-farnesol was present on LG7 (B7) but on a different chromosomal region and another on LG2 (B2). One QTL for geraniol was localized on LG5 (B5). A QTL for geranyl acetate was observed on LG2 (B2) and one for farnesal was observed on LG1 (A1). One QTL in the middle of LG5 (B5) was detected for germacrene D.

A QTL explaining 19.2% of the variability of dihydro-*β*-ionone production was located on LG4 (A4) in Y1 and one on LG6 (B6) in Y1. On LG5 (A5), one QTL for dihydro-*β*-ionol detected in Y2 and Y3 explains around 23% of the variability.

Altogether, with data from each year analyzed separately or together, we identified 84 associations accounting for the heritability of all 16 major scent compounds. QTL clusters identified as affecting rose scent may suggest common control points in biosynthetic pathways of the different scent compounds or close loci controlling the synthesis of these compounds.

Identification of *RhPAAS* as a Major Gene Linked to the Production of 2PE

In order to identify the genetic inheritance of rose scent traits, one major compound was of particular

Table 2. *Summary of QTLs for scent compounds detected with IM in the HW progeny*

The QTLs were detected in the male parent (Rw) and in the female parent (H190). Dash (–) inidcates no close MM.

QTL	Compound and Year[a]	QTL Characteristics					
		PT[b]	LG[c]	LOD Score[d]	Position[e]	MM[f]	r^2[g]
1	*E*-2-Hexenal Y1	2.5	A4	4.8	16.2	RoCol2	25.1
	E-2-Hexenal Y2	2.9	A4	6.1	17.5	–	41.0
	E-2-Hexenal Y3	2.7	A4	4.6	17.5	–	28.0
2	*E*-2-Hexenal Y1	2.6	B5	2.7	75.5	H22F01	15.0
3	*Z*-3-Hexenol Y2	2.7	A4	5.9	16.5	–	40.0
	Z-3-Hexenol Y3	2.5	A4	4.4	16.5	–	27.2
4	2PE Y1	2.5	B6	16.8	61.3	RhPAAS	63.3
	2PE Y2	3.1	B6	7.7	64.6	Rw61F2	48.8
	2PE Y3	2.7	B6	13.1	61.3	RhPAAS	62.6
5	2-Phenylacetaldehyde Y1	2.6	B6	6.3	67.5	–	31.8
6	2-Phenylethyl acetate Y2	2.6	B6	3.6	65.5	–	27.1
	2-Phenylethyl acetate Y3	2.6	B6	6.1	60.0	–	36.7
7	DMT Y3	2.6	A3	3.3	34.6	Fro9	21.3
8	DMT Y1	2.7	A5	3.1	8.0	–	17.9
9	DMT Y1	2.7	B5	4.2	16.0	–	23.4
10	Benzyl alcohol Y1	2.8	B5	5.4	16.0	–	29.0
11	Benzyl alcohol Y2	3.0	B6	4.0	64.6	Rw61F2	29.5
	Benzyl alcohol Y3	2.6	B6	5.4	58.9	–	33.3
12	Geraniol Y1	2.6	B5	2.7	27.3	EIM3.05	15.1
13	Geraniol Y1	2.6	B7	4.4	19.8	Rw5G14	23.6
	Geraniol Y2	2.8	B7	3.2	22.8	–	24.8
14	Geranyl acetate Y1	2.4	B2	3.8	19.0	H09B01f	19.1
15	Germacrene D Y1	2.5	B5	3.5	28.3	–	18.8
16	*E*-β-Farnesene Y1	2.6	B7	6.6	19.8	Rw5G14	33.4
17	Farnesal Y3	2.8	A1	3.2	45.1	RMS070	20.6
18	Farnesal Y1	2.6	B7	6.2	19.8	Rw5G14	31.8
19	*E,E*-Farnesol Y2	2.6	B2	3.1	64.0	–	25.3
20	*E,E*-Farnesol Y1	2.8	B7	11.0	19.7	–	49.2
	E,E-Farnesol Y2	2.6	B7	5.7	18.8	RwIF9	39.3
21	*E,E*-Farnesol Y3	2.7	B7	3.4	54.2	RoAP1a	21.5
22	Dihydro-β-ionone Y1	2.6	A4	2.8	27.7	–	19.2
23	Dihydro-β-ionone Y1	2.6	B6	4.1	41.8	–	22.7
24	Dihydro-β-ionol Y2	2.5	A5	3.0	31.8	RhAB38	22.7
	Dihydro-β-ionol Y3	2.5	A5	3.6	31.8	RhAB38	23.0

[a]Name of the scent compound and year (Y). [b]The threshold of the LOD score was defined by a permutation test (PT). [c]LGs are as follows: A, female map; B, male map. [d]QTLs with a LOD higher than the threshold LOD were considered. [e]Position on the linkage group (cM). [f]Closest molecular marker (MM) associated. [g]Percentage of explanation r^2.

interest and was further investigated. For 2PE, we observed a large difference between the mean and median values (Table 1). Analyses of 2PE mean contents over the 3 years showed that the progeny could be divided into two groups: group 1 with mean 2PE contents up to 2.2 μg g^{-1} fresh weight and group 2 with values from 48.3 to 498.3 μg g^{-1} fresh weight (Fig. 3). The female parent H190 produced low 2PE contents (between 1.2 and 3.2 μg g^{-1} fresh weight), while the male parent Rw produced high amounts of 2PE (between 94.5 and 183.9 μg g^{-1} fresh weight). A Pearson's χ^2 analysis was performed to test for Mendelian segregation and showed no differences between observed and expected ratios for a segregation of 1:1 ($P > 0.05$; Supplemental Table S4). This qualitative variation suggested a monogenic inheritance of this trait, which prompted us to adopt a candidate gene approach.

The biosynthesis of rose 2PE through the classical pathway described involves two steps, implicating two enzymes: RhPAAS (Kaminaga et al., 2006) and PAR (Chen et al., 2011; Fig. 1). The *PAR* gene was mapped on LG1 by Spiller et al. (2010) and localized on LG5 in the rose genome (Raymond et al., 2018). It thus cannot correspond to the QTL for 2PE content that was found on LG6. From the results of Kaminaga et al. (2006), we designed primers to isolate the *RhPAAS* gene in H190 and Rw roses (parents of the HW population). Three different alleles of the putative *RhPAAS* gene were isolated by PCR from genomic DNA. A 1,527-bp open reading frame without introns was isolated, and 22 single-nucleotide polymorphism (SNP) sites were identified in the parental genotypes (Supplemental Fig. S2). All three alleles shared 99% identity with the previously published *RhPAAS* sequence (Kaminaga et al., 2006). A comparison of the encoded 508 amino acid proteins and the published sequences from other rose cultivars confirmed the presence of a conserved Phe residue proposed to be responsible for the aldehyde

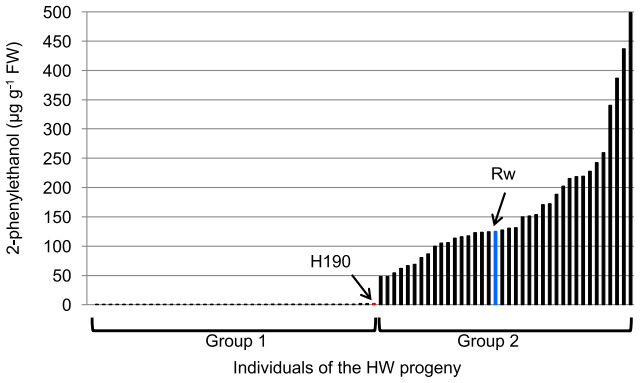

Figure 3. 2PE content in petals of Rw male parent (blue) and H190 female parent (red) and in HW progeny. Descendants were ordered according to their 2PE content. Group 1 descendants have up to 2.2 $\mu g\,g^{-1}$ fresh weight (FW) 2PE; group 2 descendants have from 48.3 to 498.3 $\mu g\,g^{-1}$ fresh weight. Values are means of three replicates, obtained during 3 successive years.

synthase activity (Supplemental Fig. S3; Torrens-Spence et al., 2013).

A single-strand conformation polymorphism (SSCP) marker allowed us to map the *RhPAAS* gene on the B6 LG (male map; Figs. 2 and 4) with a segregation ratio of 1:1 (44 versus 46). As the major QTL for 2PE was also localized on the same LG, the *RhPAAS* gene could be the locus of interest for this QTL (Fig. 2). Moreover, the SSCP electrophoresis separated *RhPAAS* PCR products into three clear bands: one for H190 (*a3* allele) and two for Rw (*a1* and *a2* alleles; Fig. 4). All individuals from the HW population that produced high amounts of 2PE (group 2) had the *a1* allele, whereas individuals producing small amounts of or no 2PE (group 1) did not, suggesting that allelic variation in *RhPAAS* could account for phenotypic variation in the HW progeny.

The amino acid sequences of the three alleles harbored eight variations, which could influence the functionality of the corresponding proteins (Supplemental Fig. S3). To test this hypothesis, we overexpressed the proteins produced by the three alleles by expressing their cDNAs in *Nicotiana benthamiana* and in the previously described somatic embryogenic callus derived from *Rosa chinensis* cv Old Blush (Vergne et al., 2010). For the transient transformation of *N. benthamiana*, leaves were infiltrated with *Agrobacterium tumefaciens* harboring *35S::RhPAAS* constructs. Stable transgenic embryogenic rose calli were recovered by using the same construct. Thirty and 15 independent transgenic events were recovered in *N. benthamiana* and rose calli, respectively. For these experiments, plants transformed with the control *p19* plasmid alone (*N. benthamiana* leaves) and untransformed rose callus explants were used as controls. Analyses of volatile compounds from transformed *N. benthamiana* leaves and rose calli showed that all three alleles were functional and able to induce the production of similar levels of 2PE (Fig. 5). The absence of 2-phenylacetaldehyde in transformed extracts suggested that this molecule was immediately converted in 2PE by an endogenous enzyme that played the role of the phenylacetaldehyde reductase (Chen et al., 2011).

Differential Expression of the Three *RhPAAS* Alleles in the HW Population

As the three proteins encoded by the three *RhPAAS* alleles had full capacity to synthesize 2PE, the causal link between the capacity to produce 2PE and the presence of *a1* allele was not a defect in one of these proteins. Differences in the expression of the three alleles in rose petals could account for variations in 2PE biosynthesis. As a first step to determine whether the *RhPAAS* gene was indeed expressed and to further characterize its expression pattern in the HW progeny, *RhPAAS* transcript accumulation was assessed during flower development by reverse transcription quantitative PCR (RT-qPCR) in the parents and in four selected individuals of the HW progeny with *a1a3* (two individuals, HW24 and HW530) and *a2a3* (two individuals, HW68 and HW149) genotypes. Non-allele-specific primers were used to measure the transcript pool abundance of *RhPAAS* in petals, the flower organs that produce the most scent. Petals were harvested from flower stages 2 to 5, and free internal pools of petal volatile compounds were collected as previously described (Bergougnoux et al., 2007). Supplemental Table S5 shows 2PE and 2-phenylacetaldehyde contents in the six individuals. During flower development, 2-phenylacetaldehyde pools followed the same trends as 2PE internal pools, the latter being generally much higher. Production of both compounds was higher at late developmental stages. Our analysis showed high expression of *RhPAAS* in the individuals producing 2PE, Rw parental line, HW24 and HW530 selected individuals (Fig. 6). In contrast, the expression was barely detectable in the lines not producing or weakly

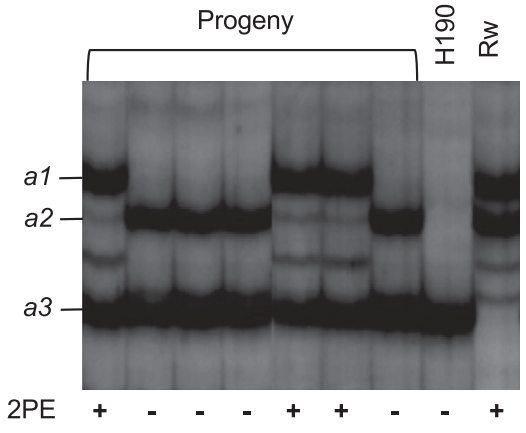

Figure 4. SSCP analysis of the *RhPAAS* gene in HW progeny. The profiles obtained for both parents (female H190 and male Rw) and several members of the progeny are shown. 2PE contents are shown (−, less than 3 $\mu g\,g^{-1}$ fresh weight; +, greater than 45 $\mu g\,g^{-1}$ fresh weight). *a1*, *a2*, and *a3* are alleles of the *RhPAAS* gene present in the HW progeny.

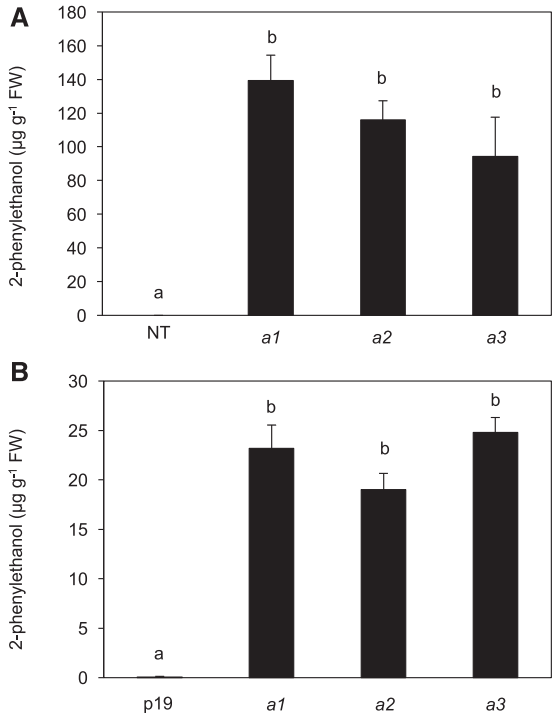

Figure 5. Overexpression of *RhPAAS* alleles in planta. A, Stable expression in *R. chinensis* cv Old Blush calli. Transformation with *A. tumefaciens* harboring the *pK7WGF2* binary vector was performed according to Vergne et al. (2010). Nontransformed plants (NT) were used as controls, and volatile compounds were extracted by hexane from calli and analyzed by GC-MS. B, Transient expression in *N. benthamiana*. *A. tumefaciens* harboring the *pK7WGF2* binary vector or the viral suppressor p19 into the *pBIN61* were mixed and coinfiltrated into the adaxial side of young leaves. Control infiltrations were performed with *A. tumefaciens* carrying the viral suppressor p19. Four days after injection, volatile compounds were extracted by hexane and analyzed by GC-MS. Error bars indicate SE obtained from 30 (*N. benthamiana* leaves) and 15 (rose calli) independent biological replicates. Means with different letters (a and b) are significantly different (Dunn's test, $P < 0.05$). FW, Fresh weight.

producing 2PE, H190 parental line, HW68 and HW149 selected individuals (Fig. 6).

Moreover, we used SNPs to elucidate allelic contribution to the *RhPAAS* expression. High-resolution melting (HRM) technology (Liew et al., 2004; McKinney et al., 2010) was used to specifically estimate allele expression in cDNAs obtained from petals at stage 2. HRM allows allele-specific detection of heterozygotes, since the PCR amplicons containing an SNP produce distinctive HRM profiles. Assuming a correct allele discrimination and using sequenced plasmids as control templates (Supplemental Fig. S4), we analyzed the allelic dosage through a comparison of cDNAs from four selected individuals (Rw, H190, HW149, and HW530). We used varying ratios of mixed plasmids as PCR templates, each containing one of the three-allele full-length cDNAs (Fig. 7; Supplemental Fig. S4). Two different SNPs were used (Supplemental Fig. S2). SNP1 was able to discriminate allele *a3* from *a1* or *a2* and SNP2 could discriminate allele *a2* from *a1* or *a3*. Used on the cDNAs, this approach confirmed the monomorphic allelic state of *a3* in the dihaploid H190 parental line, as seen in the melting curve profile (Fig. 7B; Table 3). In the *a1a2* and *a1a3* genotypes of the respective Rw parent and HW530 individual, only allele *a1* was amplified, as the melting curve profile corresponded to the *a1* control amplicon (100% of the *a1* plasmid DNA; Figure 7, A and C). This suggests that in the *a1a2* and *a1a3* genotypes, both alleles *a2* and *a3* were subjected to exclusion. In the *a2a3* HW149 progeny, although *RhPAAS* was barely expressed (Fig. 6), we could estimate that *a2* accounted for 75% and *a3* for 25% of the remaining gene expression (Fig. 7D; Table 3). In conclusion, the presence of the *a1* allele was correlated with high *RhPAAS* expression, while the other two alleles were correlated with a very weak one that did not lead to significant 2PE production. These findings are in agreement with the data obtained in the SSCP analysis.

Spatiotemporal Expression of *RhPAAS*

We observed an unexpected early expression of the gene compared with the stage of volatile 2PE production (Fig. 6). In HW individuals producing high amounts of 2PE, HW24 and HW530, *RhPAAS* expression was barely detectable at stages 4 and 5, which are the scent-production stages. In recombinant lines that produce low amounts or no 2PE, such as HW68 and HW149, the expression of *RhPAAS* was very weak, but slightly higher at stage 4. It is well known that 2PE and 1-phenylethanol can be conjugated to glycosides to be stored in the vacuoles in soluble forms (Watanabe et al., 2001; Zhou et al., 2014). To know if such forms were present in early stages of flower development in our population and explain the timing of *RhPAAS* expression, we analyzed the internal free and conjugated 2PE contents in the same samples. After incubation with a glycosidase solution, free internal volatile forms could be recovered (Fig. 8). Free internal volatile 2PE contents increased during flower development, whereas glycosylated form contents decreased, the highest being in flower buds. Moreover, 2PE free forms were present in lower quantities, irrespective of stage. These results show that 2PE is produced in the early stages of flower development through the activity of the RhPAAS enzyme and is then transformed into glycosylated soluble forms. The soluble forms are finally released at later stages. To know if this pattern of expression was specific to the *a1* allele, *RhPAAS* expression was analyzed throughout development in cv The Mac Cartney rose (Supplemental Fig. S5A). Expression was also analyzed at two stages of development (S2 and S4) in five different rose cultivars (Supplemental Fig. S5B). Early expression of the *RhPAAS* gene was confirmed in all the tested cultivars. Partial sequencing of alleles in these different rose cultivars showed high percentage identities with *a1*, *a2*, and *a3* alleles, although none of them were identical (Supplemental Fig. S6).

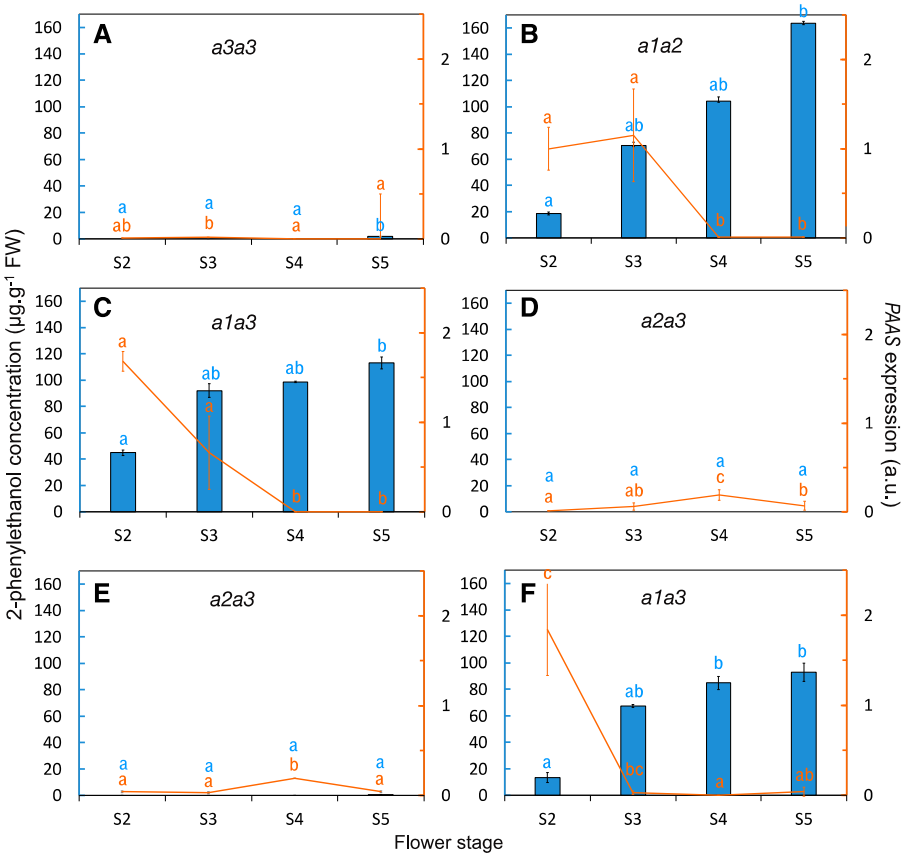

Figure 6. 2PE content analyzed by GC-MS (blue bars) and expression level of *RhPAAS* during flower development analyzed by RT-qPCR (orange lines) in the parents of the HW progeny, H190 (A) and Rw (B), and in four individuals of the progeny, HW24 (C), HW68 (D), HW149 (E), and HW530 (F). Flower developmental stages were defined by Bergougnoux et al. (2007). Transcript levels of *RhPAAS* were normalized to α-tubulin and EF1-α according to Dubois et al. (2011). Gene expression values are relative to the expression of Rw at flower stage 2, for which the value was set to 1. Error bars indicate SE obtained from three independent biological replicates. Means with different letters (a, b, and c) are significantly different (Dunn's test, $P < 0.05$). FW, Fresh weight; a.u., arbitrary units.

DISCUSSION

Scent QTLs

We performed a genetic analysis of rose scent segregation using a diploid cross from parents with contrasted scent compounds. Our study provides a comprehensive map of QTL clusters identified as affecting rose scent. QTLs were found for all main 16 volatile compounds. Thirty percent of these QTLs were stable over 2 or 3 years, whereas some were found only once (Table 2; Supplemental Tables S2 and S3). Volatile organic compound analyses to identify QTLs have not always been performed over several successive years. In a previous study on strawberry, 50% of the detected QTLs were stable over at least 2 years (Zorrilla-Fontanesi et al., 2012), whereas only about 30% were stable in our study. In *Citrus reticulata*, the percentage of stable QTLs was even less (12.14%; Yu et al., 2017). Similarly, in tomato, a large percentage of metabolites also showed variation over years (Bauchet et al., 2017). These variations might be due to differences in environmental growth conditions. Indeed, in most studies, including ours, plants were cultivated in the field under noncontrolled conditions. It was shown in raspberry that the cultivation method (open field or under tunnel) and the season greatly influenced the volatile contents and the associated QTLs (Paterson et al., 2013). As was done in apple (Costa et al., 2013) and in rose (Bourke et al., 2018), the validation of the major QTLs that we found could be done by cultivating the population in different locations or by using other segregating populations or genetic association panels. The number of QTLs detected in other studies was generally higher, probably because we focused on major volatile compounds emitted by rose cultivars and also because the two cultivars that were used are moderately scented. The availability of highly scented diploid populations limits the power of such approaches for rose. Moreover, in our study, we focused on the internal pools of volatile compounds. Analyzing the emitted volatile compounds could lead to the discovery of other QTLs, possibly related to the emission, storage, or conjugation processes.

Localizing QTLs can be used to find putative candidate genes underlying these QTLs. For example, in tomato, using both the genome sequence and transcriptomic data, Bennewitz et al. (2018) were able to propose several candidate genes for two of their identified QTLs involved in glandular trichome shapes. Although less powerful genetic tools are available in rose, putative candidate genes can sometimes be proposed using recently published genome sequences. Terpenes are very important compounds for rose scent. For example, germacrene D is a sesquiterpene frequently encountered in rose petals (Guterman et al., 2002). We found one QTL for this compound on LG5,

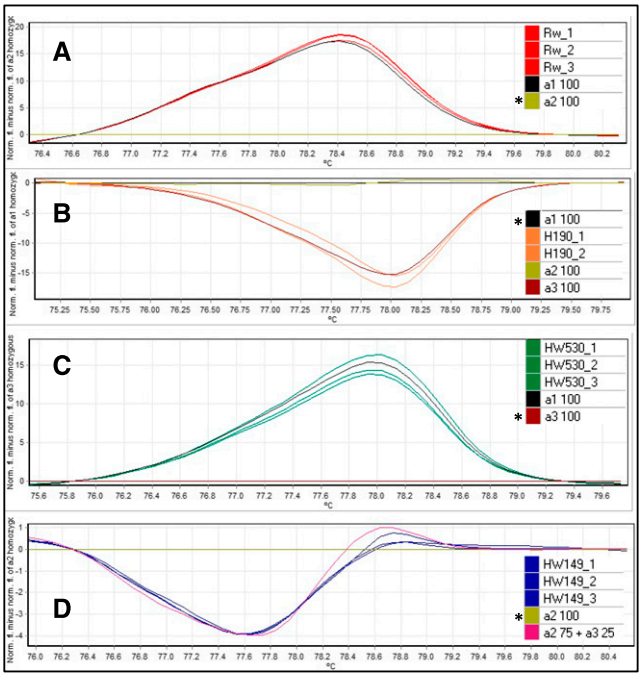

Sample	Color	Name	Genotype call	Confidence %
cDNA 1		Rw-1	a1 homozygous like	98.3
cDNA 2		Rw-2	a1 homozygous like	99.6
cDNA 3		Rw-3	a1 homozygous like	98.2
Control plasmid		a1 100	a1 homozygous	100.0
Control plasmid		a2 100	a2 homozygous	100.0
cDNA 1		H190-1	a3 homozygous like	97.5
cDNA 2		H190-2	a3 homozygous like	96.8
Control plasmid		a1 100	a1 homozygous	100.0
Control plasmid		a3 100	a3 homozygous	100.0
Control plasmid		a2 100	a2 homozygous	100.0
cDNA 1		HW530-1	a1 homozygous like	99.1
cDNA 2		HW530-2	a1 homozygous like	98.8
cDNA 3		HW530-3	a1 homozygous like	97.4
Control plasmid		a1 100	a1 homozygous	100.0
Control plasmid		a3 100	a3 homozygous	100.0
cDNA 1		HW149-1	a2a3 heterozygous 2 like	99.5
cDNA 2		HW149-2	a2a3 heterozygous 2 like	99.6
cDNA 3		HW149-3	a2a3 heterozygous 2 like	99.6
Control plasmid		a2 100	a2 homozygous	100.0
Control plasmid		a2(75)+ a3(25)	a2a3 heterozygous 2	100.0

Figure 7. HRM expression profiling of *RhPAAS*. Normalized and temperature-shifted difference plots are shown at left using a control plasmid as reference template for PCR (*). A and B, Parental genotypes. C and D, HW progeny. Two HRM primer pairs were separately used to distinguish allele-specific expression in cDNA obtained from petals at stage 2. SNP1 was used to differentiate the *a3* amplicon from the *a1/a2* amplicon in the *a3* H190 (B, orange lines) and the *a1a3* HW530 (C, green lines) backgrounds. SNP2 was used to specifically discriminate the *a2* amplicon from *a1/a3* in the *a1a2* Rw (A, red lines) and the *a2a3* HW149 (D, blue lines) backgrounds. Plasmid DNA controls were used either as pure solutions (A–C) or mixed in specific ratios to estimate allelic composition in the cDNA mixture (D; Supplemental Fig. S4). The estimated calling shown at right of expressed *RhPAAS* alleles was obtained using the genotype-calling tool of the Rotor-Gene Q Series software with a confidence of greater than 95%.

which could correspond to GERMACRENE D SYNTHASE, the terpene synthase responsible for the biosynthesis of this compound. Very recently, a *GERMACRENE D SYNTHASE* gene was annotated on chromosome 5 of the assembled rose genome (Raymond et al., 2018), thus corroborating our observation. Spiller et al. (2010) were able to identify other loci in rose that influence terpene volatile contents in an F1 progeny. One QTL for geraniol content was located on LG1. For geranyl acetate, they found a very complex inheritance pattern with four possible loci. An acetyltransferase, *RhAAT1*, was proposed as a candidate gene corresponding to one of the loci on LG2 (Shalit et al., 2003). Our study also identified a QTL for geranyl acetate in the same chromosomal region, possibly related to the presence of the same *RhAAT1* gene. Although generally present in small quantities, apocarotenoids, which are derived from carotenoid degradation, have low odor thresholds and may have a great impact on the odor of flowers such as roses (Huang et al., 2009a). In our progeny, two major apocarotenoids were produced: dihydro-β-ionone and dihydro-β-ionol. It is likely that they are derived from one another because their amounts are highly correlated in the progeny. We found three QTLs present in 1 or 2 years: two for dihydro-β-ionone on LG4 and LG6 and one for dihydro-β-ionol on LG5. In raspberry fruit, apocarotenoids were found to be the most abundant volatile compounds, and overlapping QTLs for multiple carotenoid compounds were found (Paterson et al., 2013). Enzymes involved in the biosynthesis of carotenoid derivatives are carotenoid

Table 3. *Expression of* RhPAAS *alleles* a1, a2, *and* a3 *in the parental lines and selected individuals of the HW progeny and 2PE production*

Line	2PE Production	Genotype	Allele Expression (%)		
			a1	*a2*	*a3*
Rw	+	*a1a2*	100	0	–
H190	–	*a3a3*	–	–	100
HW149	–	*a2a3*	–	75	25
HW530	+	*a1a3*	100	0	–

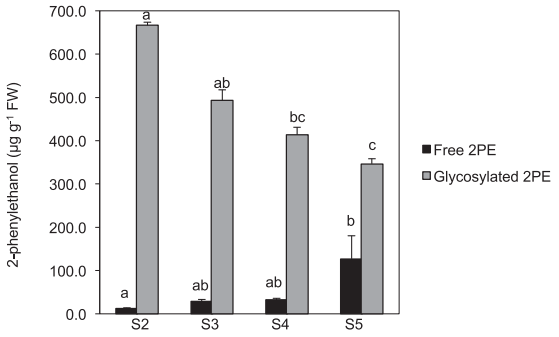

Figure 8. Evolution of free and glycosylated forms of 2PE in *R. wichurana* petals during flower development. Flower developmental stages were defined by Bergougnoux et al. (2007). Error bars indicate SE obtained from three independent biological replicates. Means with different letters (a, b, and c) are significantly different (Dunn's test, $P < 0.05$). FW, Fresh weight.

cleavage dioxygenases (CCDs), the genes encoding which are present in multiple copies in the rose genome. For example, *CCD1* has been mapped on LG1 (Spiller et al., 2010), and we found one QTL on LG1 using KW (Supplemental Table S2). *CCD4*, which is localized on LG4 (Raymond et al., 2018), could be a candidate for the QTL on the same chromosome. However, its biological role in the rose flower is still unclear (Huang et al., 2009b).

For other important scent compounds such as geraniol, no obvious gene candidate could be proposed for the QTLs we found. Geraniol production in both parents and most individuals of the progeny was very small, below 1 $\mu g\ g^{-1}$ fresh weight. Some individuals in the progeny produced higher amounts, up to 6.9 $\mu g\ g^{-1}$ fresh weight, indicating a transgressive segregation. Two QTLs were found, one on LG5 and one on LG7. It has recently been shown that the first step of geraniol biosynthesis in rose involved a nudix hydrolase, whose gene was localized on LG2 (Magnard et al., 2015). Therefore, the identified QTLs do not colocalize with this enzyme. Another step of the pathway or a regulatory protein could correspond to such QTLs. It is noteworthy that QTLs for geraniol, *E*,*E*-farnesol, farnesal, and *E*-β-farnesene were all clustered in the same chromosomic region of LG7. This could indicate that these compounds share a common biosynthetic step and/or a common regulatory gene. In tomato, it was also shown that QTLs for aroma volatile compounds derived from the same metabolic pathway were often colocalized (Saliba-Colombani et al., 2001). In rose, more transcriptomic data sets of roses with contrasting scent profiles and ultra-dense genetic maps are needed to fully exploit the QTLs that we discovered.

Involvement of RhPAAS in 2PE Production

2PE is one of the key compounds responsible for the rose odor. A cluster of QTLs was found on LG6 for 2PE as well as other phenylpropanoid-related compounds that share the same biosynthetic pathway (Fig. 1). The locus contributing to the production of 2PE was found to colocalize with one of the genes belonging to this pathway, *RhPAAS*. The corresponding enzyme catalyzes the first step in 2PE biosynthesis, having amine oxidase as well as decarboxylase activity (Kaminaga et al., 2006). We were able to show the existence of three alleles of this gene in the HW progeny. As shown by overexpression in rose calli and *N. benthamiana* leaves, the three alleles encoded perfectly functional RhPAAS isoforms. However, only genotypes having at least one copy of *a1* emitted 2PE in significant amounts. The weak accumulation of *a3* and *a2* allele transcripts certainly explains the very low production of 2PE in H190 and in the descendants with an *a2a3* genotype. To summarize, *a1*, whose transcripts are strongly accumulated, is the only allele responsible for the production of 2PE in high amounts and therefore can be considered as a dominant allele for 2PE production.

In parallel to its high expression, our data also showed an unexpected early expression of the *a1 RhPAAS* allele during flower development. The *a1* allele transcripts were accumulated at high levels just before and during the opening of the flower and were almost no longer accumulated at later stages of flowering. Although it has been reported that the expression of *RhPAAS* peaked 1 to 2 d before maximum scent emission (Farhi et al., 2010), to the best of our knowledge, the significance of the shift in expression of *RhPAAS* with respect to the emission of 2PE, which takes place at the blooming stage, has not been addressed thus far. Pioneering research on *Clarkia breweri* and *Antirrhinum majus* has shown that scent production is often regulated at the transcription level (Schnepp and Dudareva, 2006), and this seems to be a general feature of plant specialized metabolism (Colinas and Goossens, 2018). In rose, for instance, the pathway leading to the biosynthesis of DMT, partly responsible for the tea scent, has been described (Lavid et al., 2002; Scalliet et al., 2006, 2008). *O*-Methyltransferases, the enzymes that are responsible for DMT synthesis, are specifically expressed in petals of roses emitting DMT, and their expression peaks when the emission of DMT is at its maximum (Scalliet et al., 2006). However, such changes in timing of transcript accumulation between different alleles (heterochronic allelic variation) have already been shown in plants. One allele, responsible for the increase in fruit size of cultivated tomatoes, was shown to harbor such a heterochronic mutation (Frary et al., 2000; Cong et al., 2002). Our study shows that such a regulation mechanism might exist for scent-biosynthesis genes and that alleles with precocious expression might have been selected, at least in the rose cultivars that we have studied. This could have major implications for the manipulation of floral scent, which could be focused on early stages of flower development. In rose, the early expression of *RhPAAS* probably coincides with the storage of 2PE in a glycosylated form in early stages of

floral development, just after its biosynthesis. At later stages, enzymatic hydrolysis would release the compound in volatile form (Oka et al., 1999; Watanabe et al., 2001). Indeed, a β-glucosidase was partially purified from rose petals by Sakai et al. (2008). However, no gene corresponding to this enzyme has been characterized yet. In many plants, aroma compounds exist both in volatile free forms and in glycosylated forms, usually stored in vacuoles. For instance, in grape (*Vitis vinifera*), nonvolatile glycosides account for a large fraction of berries (Li et al., 2017). In tea (*Camellia sinensis*) leaves, scent compounds typically accumulate as water-soluble glycoside forms, and specific glycosyltransferases are responsible for the conjugation of various scent volatile compounds, such as geraniol, to β-primeveroside (Ohgami et al., 2015). Interestingly, a glycosyltransferase was identified as a major candidate gene for the variation of phenylacetaldehyde and 2PE contents in apple fruits (Bauchet et al., 2017). In tea leaves, two glycosyltransferases responsible for the biosynthesis of aroma β-primeverosides were characterized. It was shown that the glycosides were stored in young leaves and they were supposed to play a role in defense against herbivores, after their release upon injury. In flowers, the potential role of these storage compounds is less clear, as volatile compounds such as 2PE or geraniol are supposed to attract pollinators. Furthermore, it has been shown that 2PE attracts herbivore insects such as flower flies in the field (Imai et al., 1998). However, in case of an attack of other herbivore insects on young petals in the bud, the release of these volatile compounds could possibly play the same role of chemical defense against herbivores.

Two other QTLs for the production of 2PE have been previously described in a progeny derived from *R. multiflora* (Spiller et al., 2010). A major QTL on LG5 accounted for 60% of the variability of the trait. Using KW, we were also able to detect for 2 years a QTL for 2PE on the same LG (Supplemental Table S2). Although no sequence was provided, the authors indirectly linked this QTL to an EST whose corresponding protein was homologous to the *AMINO ACID DECARBOXYLASE RhAADC* isolated by Sakai et al. (2007). A minor QTL on LG2 accounted for 28% of the variability and was tentatively related to paralogs of the *RhAAT1 ALCOHOL ACETYLTRANSFERASE* gene (Shalit et al., 2003). RhAADC is an amino acid decarboxylase, isolated from *R.* x *hybrida* cv Hoh-Jun, with 99.8% similarity to RhPAAS reported by Kaminaga et al. (2006). The segregation patterns also differed from one another in the two populations. Fifty percent of the descendants produced significant amounts of 2PE in the HW progeny, whereas in the population studied by Spiller et al. (2010), the quantity of 2PE was nearly normally distributed. This difference is probably at the origin of the different QTLs explaining the production of this molecule. These results suggest that there are several genes encoding phenylacetaldehyde synthases on different chromosomes in rose, which could be responsible 2PE production in different segregating populations. Indeed, examination of the rose genome shows that there are multiple proteins with putative Tyr decarboxylase activities. RhPAAS, which corresponds to the QTL on LG6 and is responsible for the capacity to synthetize 2PE in our progeny, is the only one that was functionally characterized. The functions of other proteins present in the rose genome need to be studied. Moreover, it is not uncommon that QTLs for volatile compounds show a low degree of overlapping in studies on different populations in one species, as the genetic background of the parents can be different. In tomato, such lack of redundancy was attributed to environmental or methodological factors and to specific genetic variations (Rambla et al., 2017).

The gene corresponding to rose PAR, which converts phenylacetaldehyde to 2PE (Chen et al., 2011), has been localized on LG1 in the integrative genetic map (Spiller et al., 2010), while the gene is localized on LG5 in the rose genome (Raymond et al., 2018), and thus its activity does not appear to be a major limiting factor in 2PE biosynthesis in our progeny. Indeed, the expression of the rose *RhPAAS* gene in *N. benthamiana* leaves led to the production of high amounts of 2PE, but no 2-phenylacetaldehyde, suggesting that the reduction step may be supported by nonspecific endogenous reductases. An alternative pathway has been identified for the biosynthesis of 2PE in rose (Hirata et al., 2012; Fig. 1). It has been proposed that this pathway is used by the plant only in hot conditions (Hirata et al., 2016). Our plants were grown in the field and harvested during spring and summer. Our results showed that the *RhPAAS* gene was the limiting step for the production of 2PE in our progeny. Moreover, none of the genes of the alternative pathway were localized on chromosome 6. However, it would be interesting to see if the alternative pathway is turned on in the progeny under certain conditions and if it can account for some of the variations we saw in the amount of 2PE produced.

CONCLUSION

In this study, we identified a set of QTLs associated with major volatile compounds of rose. One of these QTLs was found to colocalize with a gene involved in the pathway for 2PE production, namely, *RhPAAS*, the expression of which was responsible for the capacity of descendants to produce 2PE. For the other QTLs, the identification of underlying genes and their functional characterization would be of great interest to elucidate the regulation of the levels of volatile scent compounds in rose petals. The rose genome, which has recently been published (Hibrand Saint-Oyant et al., 2018; Raymond et al., 2018), in combination with transcriptome data sets (Dubois et al., 2012; Han et al., 2017) and ultra-dense genetic maps (Bourke et al., 2017), will help assign candidate genes to the QTLs we have identified.

Moreover, these results would need to be validated in crosses involving other rose cultivars and species. Such

validation will help to better understand the genetics of rose scent and to develop molecular markers for key alleles involved in volatile biosynthesis. In addition to QTL studies, association studies, such as the ones that have already been performed on color (Schulz et al., 2016), will have to be applied on scent traits. Modern rose cultivars are tetraploids, and understanding the inheritance of desired traits is expected to be complicated (Grover et al., 2012). Finally, we observed transgressive segregations for all the analyzed compounds, with some individuals showing very high concentrations for desired scent molecules. This suggests that there are valuable genetic resources available for breeding, with the help of scent markers combined to markers for other desirable traits.

MATERIALS AND METHODS

Plant Material and Scent Analyses

The *Rosa* mapping progeny HW, as previously described (Crespel et al., 2002; Hibrand-Saint Oyant et al., 2008), consists of a full-sib family of 91 hybrids derived from a cross between a dihaploid rose, H190, obtained from haploidization of the tetraploid *Rosa* x *hybrida* cv Zambra (Meynet et al., 1994) and a hybrid of a diploid *Rosa wichurana*, Rw, originating from Jardin de Bagatelle (Paris, France). The population was planted in one copy in the field (Institut National de la Recherche Agronomique, Angers, France). *R.* x *hybrida* cv Alister Stella Gray, *Rosa* × *damascena* cv *bifera*, *R.* x *damascena* cv Kazanlik, *R.* x *hybrida* cv The Mac Cartney rose, *R.* x *hybrida* cv Papa Meilland, and *Rosa rugosa* were all cultivated outside at the University of Saint-Etienne. For the HW progeny, samples were collected during 3 successive years from 2007 to 2009 from most of the hybrids, when flowers were available. All flowers were harvested at 10 AM at stage 4 of flower development, as previously described (Bergougnoux et al., 2007). Each year, for each individual of the HW progeny, petals from different flowers of the same individual were harvested (from four to six independent flowers depending on the number of petals per flower). The petals were mixed, and two to four technical replicates were prepared by placing 1 g of petals into a glass vial for volatile compound extraction. Compounds were extracted after 24 h at 4°C with 2 mL of hexane containing 5 mg L^{-1} (±)-camphor (148075; Merck) as the internal standard. Fragrance volatile compounds were analyzed as previously described (Bergougnoux et al., 2007). The same protocol was used to analyze volatile compounds produced in *Nicotiana benthamiana* leaves and rose calli. For the analysis of 2PE glycosides, 20% (w/v) of Rw petals were crushed in citrate-phosphate buffer (pH 4.5) and centrifuged twice at 12,000*g* during 5 min. The final supernatant volume was measured (1 v) and separated into two vials (0.5 v each). In each vial, 0.5 v of the citrate-phosphate buffer was added, but in one vial, it contained the appropriate concentration of Rapidase (AR 2000; DSM) to obtain a final concentration of 20 mg mL^{-1}. Rapidase contained a mix of glycosidases, among other enzymes, from *Aspergillus niger*. After overnight incubation at 37°C, 0.25 v of hexane containing (±)-camphor was added, mixed vigorously by hand, and incubated 10 min at room temperature. The supernatant was then centrifuged twice at 10,000*g* during 10 min and analyzed by GC-MS.

Statistical and QTL Analyses

Data were analyzed using R software to determine the variance components for genotypic effect (σ_G), year interaction (σ_{GY}), and the variance between replicated samples from the same genotype (σ_{GR}). Broad-sense heritability (h^2) based on genotypic mean values averaged across years was calculated as follows (Holland et al., 2003):

$$h^2 = \sigma^2{}_G \Big/ \left(\sigma^2{}_G + \sigma^2{}_{GY}/y + \sigma^2{}_{GR}/r + \sigma^2{}_E\right)$$

where y is the number of replication years and r is the number of replication plants per genotype.

JoinMap 4.0 (Van Ooijen, 2006) was used in the construction of the linkage map. Details of the map construction are given by Hibrand-Saint Oyant et al. (2008) and Remay et al. (2009). According to the pseudo-test cross strategy (Grattapaglia and Sederoff, 1994), parental maps were separately constructed using uniparental and common biparental markers. The homologous parental linkage groups having common biparental markers were then combined, and integrated maps were constructed based on mean recombination frequencies and combined LOD scores (Van Ooijen, 2006). QTL analysis was carried out using MapQTL 5.0 (Van Ooijen, 2004). A LOD threshold at which a QTL was declared significant was determined according to a genome-wide error rate of 0.05 over 1,000 permutations (Churchill and Doerge, 1994). The Shapiro-Wilk test (Shapiro and Wilk, 1965) was applied to test normality of trait distributions. For those volatile compounds deviating from normality, several transformations (Box-Cox, Log10, and Log2) were tested without success. Because of nonnormality for most of the metabolites, the data were thus analyzed first by the nonparametric KW. A significance level of $P = 0.01$ was used as a threshold. IM was then performed with a step size of 1 cM to find regions with potential QTL effects (i.e. where the LOD score was greater than the threshold). The percentage explained by the QTL (r^2) was also presented. Other statistical analyses (normality tests, Spearman correlation tests, χ^2 tests, and Dunn's tests) were performed with XLSTAT software.

RhPAAS Isolation and Mapping on HW Populations

A forward primer for the 22 first nucleotides and two different reverse primers for the 3′ untranslated transcribed region of the published *RhPAAS* rose sequence (Kaminaga et al., 2006) were used for PCR amplification of the rose *RhPAAS* sequences from petal cDNAs and genomic DNA from the HW progeny. Forward (5′-TGTTGGAATCAACACGGAGA-3′) and reverse (5′-TCC ATTCTCACAAGCCCTTC-3′) primers were used to amplify a 597-bp cDNA fragment from six different rose cultivars. Sequences were cloned in the Stratagene StrataClone Blunt PCR cloning vector according to the manufacturer's instructions. Sequence alignments were performed using ClustalW and Geneious software. *RhPAAS* was localized on the genetic map with SSCP markers. Forward (5′-GAAAACATAGTCATGGATTGG-3′) and reverse (5′-CCGTGT TGATTCCAACAATTT-3′) primers were defined to amplify a 247-bp genomic DNA fragment. PCR was carried out in 15 μL with GoTaq Flexi DNA Polymerase according to the manufacturer's recommendations (Promega) under the following conditions: 94°C for 3 min, 40 cycles consisting of 60°C for 1 min and 72°C for 2 min, and a final elongation at 72°C for 7 min. The SSCP marker was detected as described by Remay et al. (2009).

Overexpression of *RhPAAS* in *N. benthamiana* Leaves and Rose Calli

The *RhPAAS* coding sequence was amplified and cloned into the Gateway vector pENTR/D-TOPO (Invitrogen) and then subcloned in the binary expression vector *pk7WGF2* via Gateway LR recombinant reaction between *attL* and *attR* sites for the expression in *Rosa chinensis* cv Old Blush callus (Vergne et al., 2010). *pK7WGF2* was the Ti plasmid used for the expression of the gene encoding the N-terminal GFP fusions by *CaMV35S* (Karimi et al., 2002), to allow monitoring of the transformation state of the explants. Positive clones were transformed into the *Agrobacterium tumefaciens* EHA105 strain (Hood et al., 1993). Agrobacteria cultures were used to infiltrate leaves of *N. benthamiana* as previously described (Batoko et al., 2000). Four days after infiltration, 1 g of infected leaf sectors was kept in hexane and analyzed for volatile composition as described. Rose embryogenic calli were transformed as previously described (Vergne et al., 2010), except that no transgenic rose plants were regenerated and the transformed calli were used directly for GC-MS analyses.

RNA Preparation and Gene Expression Analyses

Total RNA preparation and cDNA synthesis were performed as previously described (Dubois et al., 2011). In short, total RNA was isolated from petals of Rw, H190, four hybrids (HW24, HW68, HW149, and HW530) that were chosen based on their contrasting levels of 2PE, and six rose cultivars (*R.* x *hybrida* cv Alister Stella Gray, *R.* x *damascena* cv *bifera*, *R.* x *damascena* cv Kazanlik, *R.* x *hybrida* cv The Mac Cartney rose, *R.* x *hybrida* cv Papa Meilland, and *R. rugosa*) using the NucleoSpin RNA Plant kit (Macherey-Nagel) according to the manufacturer's instructions. After a DNase treatment performed with the Turbo DNA-free kit (Ambion), cDNA was obtained with the Revert Aid M-MulV

reverse transcriptase kit (Fermentas) at 42°C for 1 h using an oligo(dT; T11VN) primer with 1 μg of RNA. RT-qPCR was performed with the FastStart Universal SYBR Green Master (Rox; Roche Diagnostics) using the StepOnePlus real-time PCR system (Applied Biosystems). Reactions were run in duplicate and quantified against a relative standard curve prepared for a serially diluted stock cDNA containing the target sequence. Data collection and analysis were performed using the StepOne Software v2.1 (Applied Biosystems). Relative quantification of candidate genes was performed using rose orthologs of α-*TUBULIN* (GenBank accession no. AF394915) and EF1-α (GenBank accession no. BI978089) as calibrators according to Vandesompele et al. (2002). Geometric means of the arbitrary units of the calibrator's transcripts were used to normalize the relative amount of candidate gene transcripts. Primers specific to *RhPAAS* cDNAs were used for expression analysis by RT-qPCR (5′-CGTGTG GGTTCATGTGGAT-3′ and 5′-CCGAAATTCTGGACAAATGC-3′).

HRM Assay and Data Analysis

HRM assays were performed using the MeltDoctor HRM Master Mix (Applied Biosystems) according to the manufacturer's instructions. In short, primers were designed using Primer-3-Plus so as to discriminate SNP1 (G-to-A variant discriminating *a3* allele from *a1* and *a2*) and SNP2 (G-to-A variant discriminating *a2* allele from *a1* and *a3*). The primers used for SNP1 were 5′-TGAACCCATCTCAACCATCC-3′ and 5′-AGCAGTGCTAGCAGTTGAAGA G-3′, and those used for SNP2 were 5′-CGTAGAGGGCGCAAATTCTT-3′ and 5′-GGATTCGTCGACAGTGAACTTG-3′ (Supplemental Fig. S2). Relative standard curves describing PCR efficiencies for each primer pair were generated for each amplicon according to Larionov et al. (2005). HRM-qPCR amplifications were performed using 10 μL of the MeltDoctor HRM Master Mix in a 20-μL reaction volume containing 5 μM of each primer and either 10 ng μL^{-1} plasmid DNA or 1 pg μL^{-1} cDNA obtained as described earlier. PCR was performed using the Qiagen thermocycler in a 72-well rotor with the following thermal profile: 95°C for 10 min, followed by amplification for 40 cycles consisting of 95°C for 15 s and 60°C for 1 min. Amplicon dissociation was immediately started by a melting step in the same real-time PCR machine, with 0.1°C temperature increments from 60°C to 85°C. Normalization, melt calibration, and data analysis were all performed with the Rotor-Gene Q Series Software (version 2.0.2). Differences in allelic expression were estimated by using serial dilutions of plasmid DNA. The shape of the melting peaks and melting temperature values of PCR products were compared with the known dilution mixes of plasmids containing each allele (*a1*, *a2*, and *a3*; Chateigner-Boutin and Small, 2007). Triplicate technical repeats were performed with a minimum of two biological replicates.

Accession Numbers

Sequences used in this article can be found in the GenBank database under the following accession numbers: *RhPAAS a1*, MH553438; *RhPAAS a2*, MH553439; and *RhPAAS a3*, MH553440.

Supplemental Data

The following supplemental data are available.

Supplemental Figure S1. Correlation map of the quantity of volatile scent compounds found in the rose progeny.

Supplemental Figure S2. Nucleotide sequence alignment of the alleles of *RhPAAS*.

Supplemental Figure S3. Amino acid sequence alignment of the alleles of RhPAAS.

Supplemental Figure S4. HRM analysis of amplicons from plasmid DNA control mixtures.

Supplemental Figure S5. Expression level of *RhPAAS* during flower development analyzed by RT-qPCR in different rose cultivars.

Supplemental Figure S6. Partial nucleotide sequence alignment of the alleles of *RhPAAS* from different rose cultivars.

Supplemental Table S1. Estimates of broad sense heritability and different variance components.

Supplemental Table S2. Summary of QTLs for scent compounds detected with nonparametric KW in the HW progeny. The 3 year data were analyzed separately.

Supplemental Table S3. Summary of QTLs for scent compounds detected with nonparametric KW in the HW progeny. Mean values corresponding to the 3 years were considered for the scent contents.

Supplemental Table S4. Pearson's χ^2 test of 2PE contents in the HW progeny.

Supplemental Table S5. 2PE and 2-phenylacetaldehyde contents analyzed by GC-MS in the parents of the HW progeny, H190 and Rw, and in four individuals of the progeny, HW24, HW68, HW149, and HW530.

Supplemental List. Complete list of 39 compounds extracted from rose petals.

ACKNOWLEDGMENTS

We thank Nicolas Boyer, Loic Sarrabère, Isabelle Desbouchages, Priscilla Villand, and Alexis Lacroix for providing plant material. We thank the experimental unit HORTI for field plant management and the platform ANAN (Muriel Bahut) from the Structure Fédérative de Recherche Qualité et Santé du végétal for nucleic acid analysis. We thank the platform Analyse Génétique et Cellulaire of the Structure Fédérative de Recherche BioSciences Lyon (UMS3444/US8) for HRM and qPCR analyses. We thank Frédéric Hache from the English department of Saint-Etienne University for text revisions. We also thank Florence Gros, Saretta Paramita, Jérome Chameau, Sandrine Pierre, and Gilles Michel for technical assistance.

Received December 3, 2018; accepted December 20, 2018; published January 8, 2019.

LITERATURE CITED

Amrad A, Moser M, Mandel T, de Vries M, Schuurink RC, Freitas L, Kuhlemeier C (2016) Gain and loss of floral scent production through changes in structural genes during pollinator-mediated speciation. Curr Biol **26:** 3303–3312

Batoko H, Zheng HQ, Hawes C, Moore I (2000) A rab1 GTPase is required for transport between the endoplasmic reticulum and Golgi apparatus and for normal Golgi movement in plants. Plant Cell **12:** 2201–2218

Bauchet G, Grenier S, Samson N, Segura V, Kende A, Beekwilder J, Cankar K, Gallois JL, Gricourt J, Bonnet J, et al (2017) Identification of major loci and genomic regions controlling acid and volatile content in tomato fruit: Implications for flavor improvement. New Phytol **215:** 624–641

Bennewitz S, Bergau N, Tissier A (2018) QTL mapping of the shape of type VI glandular trichomes in tomato. Front Plant Sci **9:** 1421

Bergougnoux V, Caissard JC, Jullien F, Magnard JL, Scalliet G, Cock JM, Hugueney P, Baudino S (2007) Both the adaxial and abaxial epidermal layers of the rose petal emit volatile scent compounds. Planta **226:** 853–866

Bourke PM, Arens P, Voorrips RE, Esselink GD, Koning-Boucoiran CF, Van't Westende WP, Santos Leonardo T, Wissink P, Zheng C, van Geest G, et al (2017) Partial preferential chromosome pairing is genotype dependent in tetraploid rose. Plant J **90:** 330–343

Bourke PM, Gitonga VW, Voorrips RE, Visser RGF, Krens FA, Maliepaard C (2018) Multi-environment QTL analysis of plant and flower morphological traits in tetraploid rose. Theor Appl Genet **131:** 2055–2069

Chateigner-Boutin AL, Small I (2007) A rapid high-throughput method for the detection and quantification of RNA editing based on high-resolution melting of amplicons. Nucleic Acids Res **35:** e114

Chen XM, Kobayashi H, Sakai M, Hirata H, Asai T, Ohnishi T, Baldermann S, Watanabe N (2011) Functional characterization of rose phenylacetaldehyde reductase (PAR), an enzyme involved in the biosynthesis of the scent compound 2-phenylethanol. J Plant Physiol **168:** 88–95

Cherri-Martin M, Jullien F, Heizmann P, Baudino S (2007) Fragrance heritability in hybrid tea roses. Sci Hortic (Amsterdam) **113:** 177–181

Churchill GA, Doerge RW (1994) Empirical threshold values for quantitative trait mapping. Genetics **138:** 963–971

Colinas M, Goossens A (2018) Combinatorial transcriptional control of plant specialized metabolism. Trends Plant Sci **23:** 324–336

Cong B, Liu J, Tanksley SD (2002) Natural alleles at a tomato fruit size quantitative trait locus differ by heterochronic regulatory mutations. Proc Natl Acad Sci USA **99:** 13606–13611

Costa F, Cappellin L, Zini E, Patocchi A, Kellerhals M, Komjanc M, Gessler C, Biasioli F (2013) QTL validation and stability for volatile organic compounds (VOCs) in apple. Plant Sci **211:** 1–7

Crespel L, Chirollet M, Durel E, Zhang D, Meynet J, Gudin S (2002) Mapping of qualitative and quantitative phenotypic traits in *Rosa* using AFLP markers. Theor Appl Genet **105:** 1207–1214

Dubois A, Remay A, Raymond O, Balzergue S, Chauvet A, Maene M, Pécrix Y, Yang SH, Jeauffre J, Thouroude T, et al (2011) Genomic approach to study floral development genes in *Rosa* sp. PLoS ONE **6:** e28455

Dubois A, Carrere S, Raymond O, Pouvreau B, Cottret L, Roccia A, Onesto JP, Sakr S, Atanassova R, Baudino S, et al (2012) Transcriptome database resource and gene expression atlas for the rose. BMC Genomics **13:** 638–648

Dunemann F, Ulrich D, Malysheva-Otto L, Weber WE, Longhi S, Velasco R, Costa F (2012) Functional allelic diversity of the apple alcohol acyltransferase gene MdAAT1 associated with fruit ester volatile contents in apple cultivars. Mol Breed **29:** 609–625

Farhi M, Lavie O, Masci T, Hendel-Rahmanim K, Weiss D, Abeliovich H, Vainstein A (2010) Identification of rose phenylacetaldehyde synthase by functional complementation in yeast. Plant Mol Biol **72:** 235–245

François L, Verdenaud M, Fu X, Ruleman D, Dubois A, Vandenbussche M, Bendahmane A, Raymond O, Just J, Bendahmane M (2018) A miR172 target-deficient AP2-like gene correlates with the double flower phenotype in roses. Sci Rep **8:** 12912

Frary A, Nesbitt TC, Grandillo S, Knaap E, Cong B, Liu J, Meller J, Elber R, Alpert KB, Tanksley SD (2000) fw2.2: A quantitative trait locus key to the evolution of tomato fruit size. Science **289:** 85–88

Gitonga VW, Stolker R, Koning-Boucoiran CFS, Aelaei M, Visser RGF, Maliepaard C, Krens FA (2016) Inheritance and QTL analysis of the determinants of flower color in tetraploid cut roses. Mol Breed **36:** 143

Grattapaglia D, Sederoff R (1994) Genetic linkage maps of *Eucalyptus grandis* and *Eucalyptus urophylla* using a pseudo-testcross: Mapping strategy and RAPD markers. Genetics **137:** 1121–1137

Grover CE, Gallagher JP, Szadkowski EP, Yoo MJ, Flagel LE, Wendel JF (2012) Homoeolog expression bias and expression level dominance in allopolyploids. New Phytol **196:** 966–971

Guterman I, Shalit M, Menda N, Piestun D, Dafny-Yelin M, Shalev G, Bar E, Davydov O, Ovadis M, Emanuel M, et al (2002) Rose scent: Genomics approach to discovering novel floral fragrance-related genes. Plant Cell **14:** 2325–2338

Han Y, Wan H, Cheng T, Wang J, Yang W, Pan H, Zhang Q (2017) Comparative RNA-seq analysis of transcriptome dynamics during petal development in *Rosa chinensis*. Sci Rep **7:** 43382

Henz A, Debener T, Linde M (2015) Identification of major stable QTLs for flower color in roses. Mol Breed **35:** 190

Hibrand Saint-Oyant L, Ruttink T, Hamama L, Kirov I, Lakhwani D, Zhou NN, Bourke PM, Daccord N, Leus L, Schulz D, et al (2018) A high-quality genome sequence of *Rosa chinensis* to elucidate ornamental traits. Nat Plants **4:** 473–484

Hibrand-Saint Oyant L, Crespel L, Rajapakse S, Zhang L, Foucher F (2008) Genetic linkage maps of rose constructed with new microsatellite markers and locating QTL controlling flowering traits. Tree Genet Genomes **4:** 11–23

Hirata H, Ohnishi T, Ishida H, Tomida K, Sakai M, Hara M, Watanabe N (2012) Functional characterization of aromatic amino acid aminotransferase involved in 2-phenylethanol biosynthesis in isolated rose petal protoplasts. J Plant Physiol **169:** 444–451

Hirata H, Ohnishi T, Tomida K, Ishida H, Kanda M, Sakai M, Yoshimura J, Suzuki H, Ishikawa T, Dohra H, et al (2016) Seasonal induction of alternative principal pathway for rose flower scent. Sci Rep **6:** 20234

Holland JB, Nyquist WE, Cervantes-Martinez CT (2003) Estimating and interpreting heritability for plant breeding: An update. Plant Breed Rev **22:** 9–112

Hood EE, Gelvin SB, Melchers LS, Hoekema A (1993) New *Agrobacterium* helper plasmids for gene transfer to plants. Transgenic Res **2:** 208–218

Huang FC, Horváth G, Molnár P, Turcsi E, Deli J, Schrader J, Sandmann G, Schmidt H, Schwab W (2009a) Substrate promiscuity of RdCCD1, a carotenoid cleavage oxygenase from *Rosa damascena*. Phytochemistry **70:** 457–464

Huang FC, Molnár P, Schwab W (2009b) Cloning and functional characterization of carotenoid cleavage dioxygenase 4 genes. J Exp Bot **60:** 3011–3022

Imai T, Maekawa M, Tsuchiya S, Fujimori T (1998) Field attraction of *Hoplia communis* to 2-phenylethanol, a major volatile component from host flowers, *Rosa* spp. J Chem Ecol **24:** 1491–1497

Kaminaga Y, Schnepp J, Peel G, Kish CM, Ben-Nissan G, Weiss D, Orlova I, Lavie O, Rhodes D, Wood K, et al (2006) Plant phenylacetaldehyde synthase is a bifunctional homotetrameric enzyme that catalyzes phenylalanine decarboxylation and oxidation. J Biol Chem **281:** 23357–23366

Karimi M, Inzé D, Depicker A (2002) GATEWAY vectors for Agrobacterium-mediated plant transformation. Trends Plant Sci **7:** 193–195

Kawamura K, Hibrand-Saint Oyant L, Crespel L, Thouroude T, Lalanne D, Foucher F (2011) Quantitative trait loci for flowering time and inflorescence architecture in rose. Theor Appl Genet **122:** 661–675

Klahre U, Gurba A, Hermann K, Saxenhofer M, Bossolini E, Guerin PM, Kuhlemeier C (2011) Pollinator choice in Petunia depends on two major genetic loci for floral scent production. Curr Biol **21:** 730–739

Larionov A, Krause A, Miller W (2005) A standard curve based method for relative real time PCR data processing. BMC Bioinformatics **6:** 62

Lavid N, Wang J, Shalit M, Guterman I, Bar E, Beuerle T, Menda N, Shafir S, Zamir D, Adam Z, et al (2002) O-Methyltransferases involved in the biosynthesis of volatile phenolic derivatives in rose petals. Plant Physiol **129:** 1899–1907

Li XY, Wen YQ, Meng N, Qian X, Pan QH (2017) Monoterpenyl glycosyltransferases differentially contribute to production of monoterpenyl glycosides in two aromatic *Vitis vinifera* varieties. Front Plant Sci **8:** 1226

Liew M, Pryor R, Palais R, Meadows C, Erali M, Lyon E, Wittwer C (2004) Genotyping of single-nucleotide polymorphisms by high-resolution melting of small amplicons. Clin Chem **50:** 1156–1164

Linde M, Hattendorf A, Kaufmann H, Debener T (2006) Powdery mildew resistance in roses: QTL mapping in different environments using selective genotyping. Theor Appl Genet **113:** 1081–1092

Magnard JL, Roccia A, Caissard JC, Vergne P, Sun P, Hecquet R, Dubois A, Hibrand-Saint Oyant L, Jullien F, Nicolè F, et al (2015) Plant volatiles: Biosynthesis of monoterpene scent compounds in roses. Science **349:** 81–83

McKinney JT, Nay LM, De Koeyer D, Reed GH, Wall M, Palais RA, Jarret RL, Wittwer CT (2010) Mutation scanning and genotyping in plants by high-resolution DNA melting. *In* K Meksem and G Kahl,, eds, The Handbook of Plant Mutation Screening: Mining of Natural and Induced Alleles. Wiley, Weinheim, Germany, pp 149–165

Meynet J, Barrade R, Duclos A, Siadous R (1994) Dihaploid plants of roses (*Rosa* × *hybrida*, cv 'Sonia') obtained by parthenogenesis induced using irradiated pollen and in vitro culture of immature seeds. Agronomie **14:** 169–175

Ohgami S, Ono E, Horikawa M, Murata J, Totsuka K, Toyonaga H, Ohba Y, Dohra H, Asai T, Matsui K, et al (2015) Volatile glycosylation in tea plants: Sequential glycosylations for the biosynthesis of aroma β-primeverosides are catalyzed by two *Camellia sinensis* glycosyltransferases. Plant Physiol **168:** 464–477

Oka N, Ohishi H, Hatano T, Hornberger M, Sakata K, Watanabe N (1999) Aroma evolution during flower opening in *Rosa damascena* Mill. Z Naturforsch **54c:** 889–895

Paterson A, Kassim A, McCallum S, Woodhead M, Smith K, Zait D, Graham J (2013) Environmental and seasonal influences on red raspberry flavour volatiles and identification of quantitative trait loci (QTL) and candidate genes. Theor Appl Genet **126:** 33–48

Rambla JL, Medina A, Fernández-Del-Carmen A, Barrantes W, Grandillo S, Cammareri M, López-Casado G, Rodrigo G, Alonso A, García-Martínez S, et al (2017) Identification, introgression, and validation of fruit volatile QTLs from a red-fruited wild tomato species. J Exp Bot **68:** 429–442

Raymond O, Gouzy J, Just J, Badouin H, Verdenaud M, Lemainque A, Vergne P, Moja S, Choisne N, Pont C, et al (2018) The *Rosa* genome provides new insights into the domestication of modern roses. Nat Genet **50:** 772–777

Remay A, Lalanne D, Thouroude T, Le Couviour F, Hibrand-Saint Oyant L, Foucher F (2009) A survey of flowering genes reveals the role of gibberellins in floral control in rose. Theor Appl Genet **119:** 767–781

Roman H, Rapicault M, Miclot AS, Larenaudie M, Kawamura K, Thouroude T, Chastellier A, Lemarquand A, Dupuis F, Foucher F, et al (2015) Genetic analysis of the flowering date and number of petals in rose. Tree Genet Genomes **11:** 85

Sakai M, Hirata H, Sayama H, Sekiguchi K, Itano H, Asai T, Dohra H, Hara M, Watanabe N (2007) Production of 2-phenylethanol in roses as the dominant floral scent compound from L-phenylalanine by two key enzymes, a PLP-dependent decarboxylase and a phenylacetaldehyde reductase. Biosci Biotechnol Biochem **71:** 2408–2419

Sakai M, Tomita S, Hirata H, Asai T, Dohra H, Hara M, Watanabe N (2008) Purification and characterization of β-glucosidase involved in the emission of 2-phenylethanol from rose flowers. Biosci Biotechnol Biochem **72:** 219–221

Saliba-Colombani V, Causse M, Langlois D, Philouze J, Buret M (2001) Genetic analysis of organoleptic quality in fresh market tomato. 1. Mapping QTLs for physical and chemical traits. Theor Appl Genet **102:** 259–272

Scalliet G, Lionnet C, Le Bechec M, Dutron L, Magnard JL, Baudino S, Bergougnoux V, Jullien F, Chambrier P, Vergne P, et al (2006) Role of petal-specific orcinol O-methyltransferases in the evolution of rose scent. Plant Physiol **140:** 18–29

Scalliet G, Piola F, Douady CJ, Réty S, Raymond O, Baudino S, Bordji K, Bendahmane M, Dumas C, Cock JM, et al (2008) Scent evolution in Chinese roses. Proc Natl Acad Sci USA **105:** 5927–5932

Schnepp J, Dudareva N (2006) Floral scent: Biosynthesis, regulation and genetic modifications. *In* C Ainsworth, ed, Annual Plant Reviews 20: Flowering and Its Manipulation. Blackwell Publishing, Oxford, UK, pp 240–257

Schulz DF, Schott RT, Voorrips RE, Smulders MJM, Linde M, Debener T (2016) Genome-wide association analysis of the anthocyanin and carotenoid contents of rose petals. Front Plant Sci **7:** 1798

Shalit M, Guterman I, Volpin H, Bar E, Tamari T, Menda N, Adam Z, Zamir D, Vainstein A, Weiss D, et al (2003) Volatile ester formation in roses: Identification of an acetyl-coenzyme A. Geraniol/Citronellol acetyltransferase in developing rose petals. Plant Physiol **131:** 1868–1876

Shapiro SS, Wilk MB (1965) An analysis of variance test for normality (complete samples). Biometrika **52:** 591–611

Souleyre EJ, Chagné D, Chen X, Tomes S, Turner RM, Wang MY, Maddumage R, Hunt MB, Winz RA, Wiedow C, et al (2014) The AAT1 locus is critical for the biosynthesis of esters contributing to 'ripe apple' flavour in 'Royal Gala' and 'Granny Smith' apples. Plant J **78:** 903–915

Spiller M, Berger RG, Debener T (2010) Genetic dissection of scent metabolic profiles in diploid rose populations. Theor Appl Genet **120:** 1461–1471

Tieman D, Zhu G, Resende MFR Jr, Lin T, Nguyen C, Bies D, Rambla JL, Beltran KSO, Taylor M, Zhang B, et al (2017) A chemical genetic roadmap to improved tomato flavor. Science **355:** 391–394

Torrens-Spence MP, Liu P, Ding H, Harich K, Gillaspy G, Li J (2013) Biochemical evaluation of the decarboxylation and decarboxylation-deamination activities of plant aromatic amino acid decarboxylases. J Biol Chem **288:** 2376–2387

Vandesompele J, De Preter K, Pattyn F, Poppe B, Van Roy N, De Paepe A, Speleman F (2002) Accurate normalization of real-time quantitative RT-PCR data by geometric averaging of multiple internal control genes. Genome Biol **3:** H0034

Van Ooijen JW (2004) MapQTL 5.0 Software for the Mapping of Quantitative Trait Loci in Experimental Populations. Plant Research International, Wageningen, The Netherlands

Van Ooijen JW (2006) JoinMap 4.0 Software for the Calculation of Genetic Linkage Maps in Experimental Populations. Plant Research International, Wageningen, The Netherlands

Vergne P, Maene M, Gabant G, Chauvet A, Debener T, Bendahmane M (2010) Somatic embryogenesis and transformation of the diploid *Rosa chinensis* cv Old Blush. Plant Cell Tissue Organ Cult **100:** 73–81

Vogt J, Schiller D, Ulrich D, Schwab W, Dunemann F (2013) Identification of lipoxygenase (LOX) genes putatively involved in fruit flavour formation in apple (*Malus* × *domestica*). Tree Genet Genomes **9:** 1493–1511

Watanabe S, Hashimoto I, Hayashi K, Yagi K, Asai T, Knapp H, Straubinger M, Winterhalter P, Watanabe N (2001) Isolation and identification of 2-phenylethyl disaccharide glycosides and mono glycosides from rose flowers, and their potential role in scent formation. Biosci Biotechnol Biochem **65:** 442–445

Yan Z, Visser PB, Hendriks T, Prins TW, Stam P, Dolstra O (2007) QTL analysis of variation for vigour in rose. Euphytica **154:** 53–62

Yauk YK, Chagné D, Tomes S, Matich AJ, Wang MY, Chen X, Maddumage R, Hunt MB, Rowan DD, Atkinson RG (2015) The O-methyltransferase gene MdoOMT1 is required for biosynthesis of methylated phenylpropenes in ripe apple fruit. Plant J **82:** 937–950

Yauk YK, Souleyre EJF, Matich AJ, Chen X, Wang MY, Plunkett B, Dare AP, Espley RV, Tomes S, Chagné D, et al (2017) Alcohol acyl transferase 1 links two distinct volatile pathways that produce esters and phenylpropenes in apple fruit. Plant J **91:** 292–305

Yu Y, Bai J, Chen C, Plotto A, Yu Q, Baldwin EA, Gmitter FG Jr (2017) Identification of QTLs controlling aroma volatiles using a 'Fortune' × 'Murcott' (*Citrus reticulata*) population. BMC Genomics **18:** 646

Zhou Y, Dong F, Kunimasa A, Zhang Y, Cheng S, Lu J, Zhang L, Murata A, Mayer F, Fleischmann P, et al (2014) Occurrence of glycosidically conjugated 1-phenylethanol and its hydrolase β-primeverosidase in tea (*Camellia sinensis*) flowers. J Agric Food Chem **62:** 8042–8050

Zini E, Biasioli F, Gasperi F, Mott D, Aprea E, Mark TD, Patocchi A, Gessler C, Komjanc M (2005) QTL mapping of volatile compounds in ripe apples detected by proton transfer reaction-mass spectrometry. Euphytica **145:** 269–279

Zorrilla-Fontanesi Y, Rambla JL, Cabeza A, Medina JJ, Sánchez-Sevilla JF, Valpuesta V, Botella MA, Granell A, Amaya I (2012) Genetic analysis of strawberry fruit aroma and identification of O-methyltransferase FaOMT as the locus controlling natural variation in mesifurane content. Plant Physiol **159:** 851–870